6 SCIENTIFIC HIGHLIGHT OF THE MONTH: Diluted Magnetic Semiconductors

Dilute Magnetic Semiconductors

K. Sato and H. Katayama-Yoshida
ISIR, Osaka University, 567-0047 Osaka, Japan
P. H. Dederichs
IFF, Research Center Jülich, D-52425 Jülich, Germany

Abstract

We describe exchange interactions in dilute magnetic semiconductors (DMS) based on ab-initio calculations. Electronic structure of DMS is calculated on the basis of the density functional theory by using the Korringa-Kohn-Rostoker coherent potential approximation (KKR-CPA). We will show that there are two classes of DMS with very different properties. In systems with localised majority d-states deep in the valence band, the ferromagnetism is induced by Zener's p-d exchange interaction. This interaction is weak but long ranged. For systems with impurity-bands in the gap, the ferromagnetism is driven by Zener's double exchange mechanism. This interaction is very strong but short ranged. Sophisticated Monte Carlo methods show that for small concentrations the percolation effect should be included to estimate Curie temperatures of DMS. In particular, the ferromagnetism is strongly suppressed in double exchange systems due to the absence of the percolation for low concentrations.

1 Introduction

Half-metals are considered to be the ideal materials for spintronics. They are particular ferromagnets which from electronic structure point of view can be considered as hybrids between metals and semiconductors, since the majority density of states is metallic, i.e., finite at the Fermi level E_{F}, while the minority bands exhibit a gap at E_{F}. Therefore at E_{F} a 100 % spin polarisation exists, which is ideal for the efficiency of spin dependent devices [1, 2].

Since the discovery of half-metallicity in the Heusler alloys by de Groot [3], many other materials like certain manganites, e.g., $La_{0.7}Sr_{0.3}MnO_3$ [4], double perovskites, e.g., Sr_2FeReO_6 [5] as well as the transition metal oxides CrO_2, Fe_2O_3 [4] have been shown to be half-metals. To this class also belong dilute magnetic semiconductors (DMS), such as $In_{1-x}Mn_xAs$ and $Ga_{1-x}Mn_xAs$ discovered by Munekata et al. [6] and Ohno et al. [7]. In these systems a small concentration of

Mn atoms, or in general of transition metal atoms (TM), with typical concentrations of 3 - 8 %, are randomly distributed on the cation sites. Due to the small concentrations the systems behave structurally as semiconductors and can be easily grown on the corresponding parent substrate, i.e., (Ga, Mn)As on GaAs. Moreover they can be doped and manipulated as semiconductors, which offers a large prospect for applications. However a problem of these DMS-systems is, that the Curie temperatures are well below room temperature, e.g., 170 K for (Ga, Mn)As, representing the best investigated system. This is the major obstacle for applications [1, 2, 8].

In this paper, we will discuss the basic electronic structure of dilute magnetic semiconductors. We will concentrate on the magnetic properties, in particular the exchange mechanism which control the ferromagnetism in these systems. Moreover we present calculations of the Curie temperatures based (i) on the most simple mean-field approximation and (ii) on sophisticated Monte Carlo methods. The ab-initio calculations are performed within the density functional formalism by using the Korringa-Kohn-Rostoker (KKR) method together with the coherent potential approximation (CPA) to describe the disorder in these systems. As a result we will show that there are two classes of DMS, one, in which the majority d-states are well localised below the valence band, and a second one, where impurity d-bands in the gap exist. In the former class the interaction is dominated by Zener's p-d exchange being relatively weak, but longer ranged, while in the latter one Zener's double exchange prevails, being strong but short ranged. Both have important consequences for the Curie temperatures.

2 Ab-initio Calculations for Dilute Magnetic Semiconductors

The results presented in this review are obtained by ab-initio calculations based on density functional theory (DFT). Exchange and electronic correlation effects are described by the local density approximation, the standard working horse in the field. As calculational method we use the KKR-Green function method. Green function methods avoid the calculation of eigenfunction ϕ_α and eigenvalues E_α of the Kohn-Sham equations of DFT. The Green function $G(\boldsymbol{r}, \boldsymbol{r}'; E)$, defined as the causal solution of the Kohn-Sham equation with a unit source term at the position $\mathbf{r}'$

$$(-\frac{\hbar^2}{2m}\nabla^2 + V(\boldsymbol{r}) - E)G(\boldsymbol{r}, \boldsymbol{r}'; E) = -\delta(\boldsymbol{r} - \boldsymbol{r}') \tag{1}$$

allows to determine the charge density $n(\boldsymbol{r})$ directly from its imaginary part by integrating over all occupied states

$$n(\boldsymbol{r}) = -\frac{2}{\pi}\int^{E_\mathrm{F}} dE \mathrm{Im}G(\boldsymbol{r}, \boldsymbol{r}; E) \tag{2}$$

and the density of states (DOS) in a certain volume V by a volume integral

$$n(E) = -\frac{2}{\pi}\int_V d\boldsymbol{r} \mathrm{Im}G(\boldsymbol{r}, \boldsymbol{r}; E) \tag{3}$$

The KKR method is based on multiple scattering theory which is of strong advantage for the description of the disorder introduced by the transition metal impurities like Mn, which are

randomly distributed on the cation sites, i.e., on the Ga sites in GaAs. Therefore this disorder corresponds to the disorder in a random A_cB_{1-c} alloy where $c = c_A$ denotes the concentration of A atoms and $c_B = 1 - c_A$ the one of B atoms. This disorder problem can be well described by the coherent potential approximation (CPA) [9], in which the atoms A and B are embedded in an effective 'CPA'-medium which is determined selfconsistently. If we denote the atomic t-matrices of the A- and B-atoms and of the CPA medium by t_A, t_B and t_{CPA}, then the CPA selfconsistency condition, which determine t_{CPA}, leads in the multiple scattering KKR description to

$$c_A T_A + c_B T_B = 0 \tag{4}$$

where $T_{A,B}$ describes the total single-site T-matrix of an atom A or B embedded in the CPA medium on site 0

$$T_A = (t_A - t_{CPA}) \frac{1}{1 - G^{00}_{CPA}(t_A - t_{CPA})} \tag{5}$$

where G^{00}_{CPA} are the on-site elements of the CPA Green function G_{CPA} at site 0. These elements can be calculated from t_{CPA} by Brillouin zone integration

$$G_{CPA} = \frac{1}{V_{BZ}} \int_{BZ} d\boldsymbol{k} g(\boldsymbol{k}) \frac{1}{1 - t_{CPA} g(\boldsymbol{k})} \tag{6}$$

where $g(\boldsymbol{k})$ are the free space structure constants.

According to eq. (5) the CPA medium, i.e., the CPA-scattering matrix t_{CPA}, has to be chosen such that on the statistical average the insertion of an A and B atom at the considered site into the CPA medium does not change the scattering which is the condition of eq. (4). In our calculations we used the KKR-CPA code MACHIKANEYAMA 2000 produced by H. Akai of Osaka University [10].

All the above considerations can be easily generalised to the case of a spin polarised system where we have to distinguish two charge densities $n^+(\boldsymbol{r})$ and $n^-(\boldsymbol{r})$, where $n(\boldsymbol{r}) = n^+ + n^-$ and $m(\boldsymbol{r}) = n^+ - n^-$ are the charge- and magnetisation-densities. All quantities G, t_A, t_B, T_A etc. have then an additional spin index. For dilute magnetic semiconductors it is very important to distinguish two states, the ferromagnetic one, where all moments of the magnetic atoms are aligned in one direction, or the disordered-local-moment (DLM) state (or spin-glass state) where the directions of all local moments are randomly distributed, so that the average magnetisation vanishes. While the description of the ferromagnetic states is straightforward in the above CPA formalism, the DLM state can be considered as a three component alloy, where in addition to the Ga atoms with concentration $1 - c$, the Ga sites are occupied either with Mn atoms with local moment 'up' ($Mn^{\uparrow}$) or with Mn atoms with moment 'down' ($Mn^{\downarrow}$), both with equal concentrations $c/2$ [9].

To evaluate the thermodynamic properties, we describe the system by a classical Heisenberg model

$$H = -\frac{1}{2} \sum_{i \neq j} J_{ij} \vec{M}_i \cdot \vec{M}_j \tag{7}$$

where $\vec{M}_i$ and $\vec{M}_j$ denote the local moments, in particular their directions, of the magnetic impurities i and j and J_{ij} the exchange integral between these atoms. This we calculated by the formula of Liechtenstein [11], which describes the energy change due to a small change of the angle between both moments within the frozen potential approximation.

$$J_{ij} = \frac{1}{4\pi}\mathrm{Im}\int^{E_\mathrm{F}} dE \mathrm{Tr}\{(t_i^+ - t_j^-)G_{ij}^+(E)(t_i^+ - t_j^-)G_{ji}^-(E)\} \tag{8}$$

$t_i^\pm$ is the atomic t-matrix of atom i for majority(+) and minority(-) spin directions and $G_{ij}^\pm$ is the Green function of the system.

The disorder of the other atoms is described by identifying the Green function $G_{ij}^\pm$ between i and j by the Green function of the ferromagnetic CPA medium. The exchange coupling constants J_{ij} describe not only the sign and the strength of the coupling, but also their spatial extent, which is particular important for the considered diluted systems.

Given the J_{ij}, the thermodynamic properties and in particular the Curie temperature T_C can be described by standard statistical methods. In the simplest mean-field approximation (MFA) the action of all neighbors j of impurity i is calculated by an average field

$$H_i = c\sum_{j(\neq i)} J_{ij}\langle M_j\rangle \tag{9}$$

where $\langle M\rangle = \langle M_j\rangle = \langle M_i\rangle$ is the average moment and c the occupation probability for site j. The condition of vanishing $\langle M\rangle$ then yields as Curie temperature in MFA

$$k_\mathrm{B}T_\mathrm{C}^\mathrm{MFA} = \frac{1}{3}cM^2\sum_{j(\neq i)} J_{ij} \tag{10}$$

Note that in MFA only the sum of all J_{ij} enters, but not the spatial extent. Therefore the mean-field value $T_\mathrm{C}^\mathrm{MFA}$ can also be calculated directly from the CPA total energies for the ferromagnetic ground state E_FM and from the disordered local moment state E_DLM. In the mean-field approximation of the Heisenberg model the ground state energy H_DLM vanishes for the DLM states

$$H_\mathrm{DLM} = -\frac{1}{2}\sum_{i\neq j} J_{ij}\langle M_i\rangle\cdot\langle M_j\rangle = 0 \tag{11}$$

since the average moments $\langle M_i\rangle$ vanish due to the average over all directions. On the other hand for the ferromagnetic ground state one obtains:

$$H_\mathrm{FM} = -\frac{1}{2}c^2M^2\sum_{i\neq j} J_{ij} \tag{12}$$

Since orientational degrees of freedom should be described well by the Heisenberg model, we can identify the difference

$$H_\mathrm{DLM} - H_\mathrm{FM} = E_\mathrm{DLM}^\mathrm{CPA} - E_\mathrm{FM}^\mathrm{CPA} \tag{13}$$

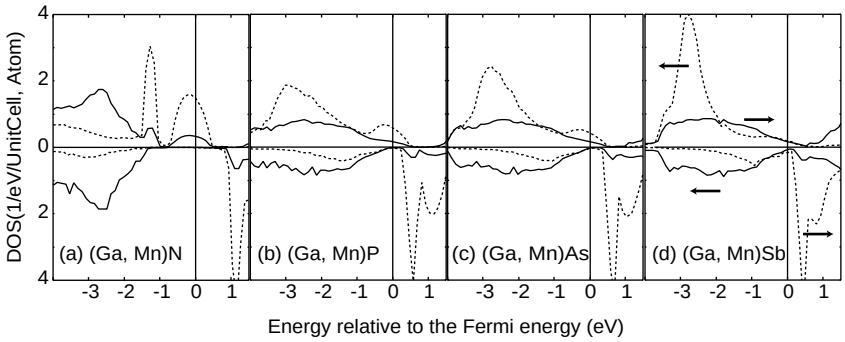

Figure 1: Density of states of dilute magnetic semiconductors with 5 % Mn impurities: (a) (Ga, Mn)N, (b) (Ga, Mn)P, (c) (Ga, Mn)As and (d) (Ga, Mn)Sb. The full curve gives the average DOS of the whole system, the dotted curve the local DOS of the Mn atoms.

by the total energy difference for the ferromagnetic system, e.g., $Ga_{1-c}Mn_c^{\uparrow}As$, and the DLM system with 50 % Mn moments up and 50 % down, i.e., $Ga_{1-c}Mn_{c/2}^{\uparrow}Mn_{c/2}^{\downarrow}As$. By comparison with the above result for T_C^{MFA} we obtain then

$$k_B T_C^{MFA} = \frac{2}{3} \frac{E_{DLM}^{CPA} - E_{FM}^{CPA}}{c} \tag{14}$$

Thus in MFA the Curie temperature is determined by the total energy difference per Mn atom between the DLM and FM state [12].

Often the MFA does not give reliable results. In this case Monte Carlo simulations offer an (numerically) exact method to calculate the thermodynamic properties. For details see Sect. 5.

3 Local Density of States and Curie Temperatures in MFA

Here we present results of ab-initio calculations for a series of III-V DMS with 5 % Mn impurities. We have chosen the sequence (Ga, Mn)N, (Ga, Mn)P, (Ga, Mn)As and (Ga, Mn)Sb, where only the anions N, P, As and Sb are different. For the results it is most important that the majority d-level of Mn has a lower energy than the atomic p-level of Sb, but a higher energy than the p-level of N, while the p-levels of P and As are intermediate.

Fig. 1 shows the density of states (DOS) for the considered systems with 5 % Mn on the Ga sites. The upper curves refers to the majority DOS, the lower inverted ones to the minority DOS, both for the ferromagnetic configuration. The full curves show the average total density of states of the DMS with 5 % Mn. Due to the small concentration of Mn this is roughly the DOS of the pure semiconductors, consisting of the occupied valence band, dominated by the anion p-states and the empty conduction band, formed mostly by the Ga s-states. The dotted lines show the local DOS of the Mn atoms. We consider only the neutral charge state without additional dopants. Since Mn has 7 valence electrons and substitutes for a Ga atom, 3 of the 7 electrons can replace the 3 Ga electrons in the valence band. The remaining 4 electrons have to be put in new localised d-states in the band gap. Therefore the electronic structure of transition metal impurities in semiconductors is dominated by d-states in the gap, which for finite concentrations develop into impurity bands. Since Mn has a large moment, only the majority states are occupied leading

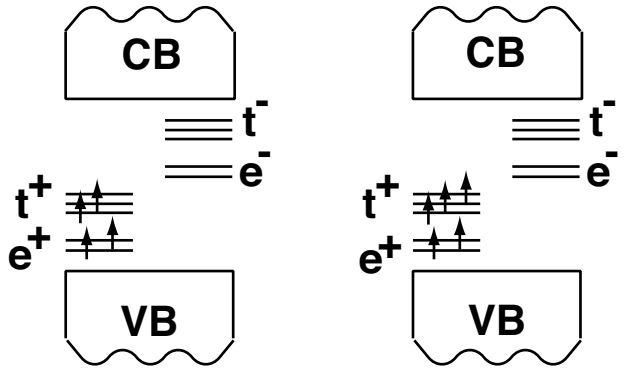

Figure 2: Impurity levels of magnetic transition metal impurities in semiconductors: For Mn on the III-site in III-V semiconductors the double degenerate e^+ state and two of the three degenerate t^+ states are occupied (left figure); the same states are occupied for Cr impurities on II-sites in II-VI semiconductors. On the other hand for Mn impurities in II-VI and Fe impurities in III-V semiconductors all five majority states (right figure) are occupied.

to a so-called 'high-spin state'. The impurity levels are schematically indicated in Fig. 2. Two different impurity levels have to be distinguished: A twofold degenerate e-state ($d_{z^2}, d_{x^2-y^2}$), the wave functions of which for symmetry reasons hybridize very little with the valence band p-states, and a threefold degenerate t-state (d_{xy}, d_{yz}, d_{zx}) which strongly hybridizes with the p-states, resulting in bonding- and antibonding hybrides. While the bonding hybrides are located in the valence band, the antibonding hybrides form the impurity t-states in the gap, which are due to the hybridization shifted to higher energies than the e-states. In the neutral configuration only the two e-states and two of the three t-states in the majority band are occupied, while the minority gap states are empty.

In Fig. 1 both the e- and t-states can be very well seen for the GaN compound with 5 % Mn. Since the d-states around the individual Mn atoms overlap and form an impurity band, the higher and broader band corresponds to the more extended t-states, and the lower narrow one to the more localised e-states. Within the valence band there is also some hybridised-in Mn DOS from the bonding t-hybrides. The Fermi level falls into the majority t-impurity band, such that per Mn atom exactly two e-states and two t-states are occupied, leaving one majority t-state and all minority d-states empty. Therefore the considered system is a half-metallic ferromagnet, with a moment of 4 μ_{B} per Mn atom.

When we move from Mn in GaN to Mn in GaP and GaAs we notice that the Mn d-level is shifted to lower energies. For (Ga, Mn)P the e-state has fully moved in the valence band, while the t-state forms with the valence p-states of the P atom a resonance at E_{F}. Most of the local d-intensity of the Mn atom is now located at the bonding t-states within the valence band. For (Ga, Mn)As these trends are even somewhat stronger. Finally for (Ga, Mn)Sb, the resonance at the Fermi level has more or less disappeared, such that at E_{F} the local Mn DOS agrees well with the DOS of the Sb atoms. Since the minority d-like gap states are in all cases unoccupied, the total moment is fixed to 4 μ_{B} per Mn. However in the case of (Ga, Mn)Sb the situation is very different from (Ga, Mn)N, since in GaSb all 5 majority d-states are occupied, while a hole exist in the Sb majority p-states at the Fermi level. Therefore the filling of the five d-resonances leads to a total moment of 5 μ_{B}, which is, however, reduced to 4 μ_{B} per Mn atom by the empty states in

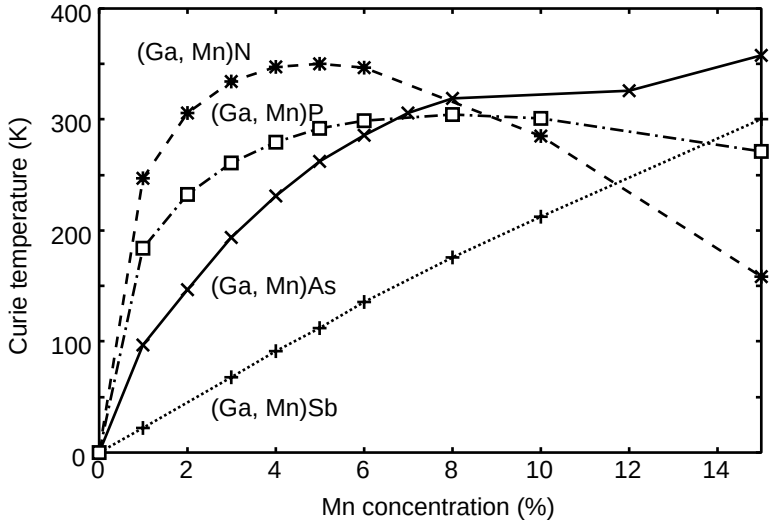

Figure 3: Curie temperatures of Mn doped III-V semiconductors, as calculated in the mean field approximation as a function of the Mn concentration.

the majority p-band. Thus in the CPA description the Sb atoms are weakly and homogeneously polarised, with an average moment of -1 $\mu_{\rm B}$ per Mn atom, being antiferromagnetically coupled to the Mn moments, such that the total moment per Mn atom is still 4 $\mu_{\rm B}$. In summary the behaviour of Mn in GaN and GaSb is completely different. In fact, both systems represent two extremes: in (Ga, Mn)N the d-states are in the gap and form impurity bands at $E_{\rm F}$, while in (Ga, Mn)Sb the d-states are at the lower end of the valence band and fully occupied, while a hole exist in the majority valence band. The behaviour of Mn in GaP and GaAs lies between these two extremes. In all cases the minority d-states are unoccupied.

The Curie temperatures $T_{\rm C}$, calculated in MFA for these systems, reflect this strongly different behaviour. Fig. 3 shows the calculated $T_{\rm C}^{\rm MFA}$ values for the four systems as a function of the concentration c of Mn impurities. For (Ga, Mn)Sb we find a linear dependence on the concentration, but in the other cases a strong non-linear dependence is obtained, which is particular pronounced for (Ga, Mn)N. As we will demonstrate below, in this case $T_{\rm C}^{\rm MFA}$ scales as the square root of the concentration c, leading to very large $T_{\rm C}$ values already for small concentrations of Mn. The behaviour of (Ga, Mn)As is intermediate between these extremes: a weaker $\sqrt{c}$-dependence for smaller concentrations and a linear dependence for larger concentrations. As we will discuss in the following, the different concentration dependences are caused by two different exchange mechanisms, which stabilize the ferromagnetism, i.e., double exchange in the case of impurity bands in the gap and kinetic or p-d exchange in the case of nearly localised d-levels below the valence band [13].

4 Double Exchange, Super Exchange and Kinetic p-d Exchange

To identify the exchange mechanism, which stabilises ferromagnetism or antiferromagnetism, is an important problem in magnetic materials. For dilute magnetic semiconductors this means identifying the mechanism which stabilises the ferromagnetism already for small concentrations [12, 13, 14].

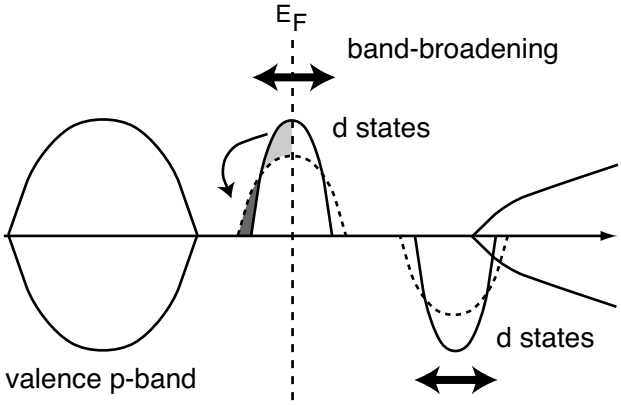

Figure 4: Double exchange: Due to the broadening of the impurity t-band with increasing Mn concentration c, states are transferred to lower energies, leading to an energy gain, if the Fermi energy lies in the band. As explained in the text, the band width increases as $\sqrt{c}$.

For (Ga, Mn)N the characteristic features of the DOS of the ferromagnetic state is sketched in Fig. 4. The Fermi energy lies in the majority impurity band of t-symmetry. The important energy gain arises from the broadening of the impurity band with increasing concentration c. If we increase the concentration from a lower value, with the DOS given by the full line, to a larger value corresponding to the broader DOS as given by the dashed line, we transfer DOS-weight from around $E_{\rm F}$ to lower energies, leading to an energy gain, which, as we will show, stabilises the ferromagnetic state. This energy gain is proportional to the band width W of the impurity band, which scales as the square root $\sqrt{c}$ of the concentration. The energy gain due to band broadening is known as Zener's double exchange [14].

This can be proven by a theorem for tight-binding model. The square of the band width is given by the energy variance

$$W^2 = \overline{(E - \bar{E})^2} = \sum_{m \neq 0} |H_{0m}|^2 \tag{15}$$

which itself is determined by the sum of the hopping probabilities $|H_{0m}|^2$ from site 0 to any other site m. H_{0m} is the so-called hopping matrix element. Consider now a disordered lattice with a random distribution of Mn atoms. Starting from a given Mn atom at site 0, an electron can only hop from the state centered at 0 to the site m, if this site is occupied by another Mn atom. If we denote the Mn-Mn hopping integral by t_{0m}, we find in the disordered system

$$H_{0m} = t_{0m}(\text{if Mn atom at m}) \text{ or } 0(\text{otherwise}) \tag{16}$$

By averaging over all configurations of Mn atoms we therefore obtain

$$\langle W^2 \rangle_{\rm conf} = \sum_{m \neq 0} \langle |H_{0m}|^2 \rangle = c \sum_{m \neq 0} |t_{0m}|^2 \tag{17}$$

since the probability to find a Mn atom at site m is given by the atomic concentration c. Thus the effective band width $W_{\rm eff}$ scales as $\sqrt{c}$. This $\sqrt{c}$ behaviour of band width can be clearly

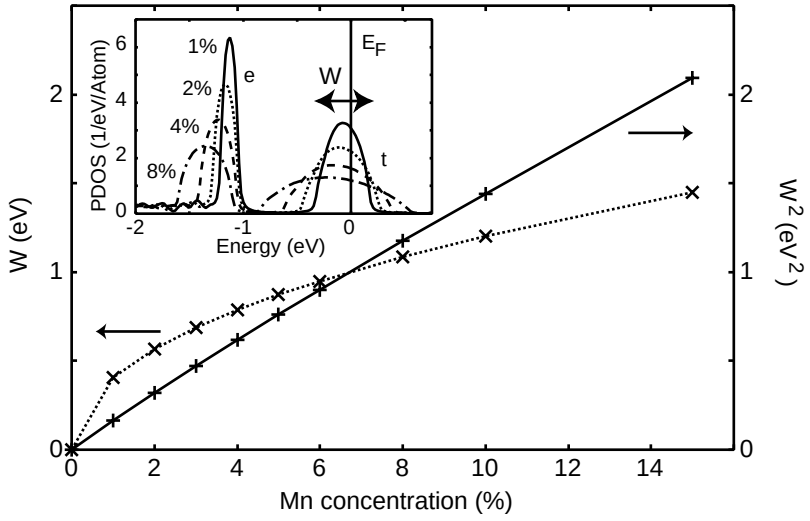

Figure 5: Impurity band width W and its square W^2 for the impurity t-band in (Ga, Mn)N as a function of Mn concentration. The inset shows the local density of Mn gap states.

seen in calculated DOS as is shown in Fig. 5. In the figure W and its square are plotted as a function of Mn concentration. The linear dependence of W^2 on Mn concentration indicates a $\sqrt{c}$ dependence of W. Thus, the energy gain of the ferromagnetic state with increasing concentration scales as $\sqrt{c}$, which explains the strong increase of the Curie temperature in MFA as shown in Fig. 3 for (Ga, Mn)N. The double exchange mechanism is only important, if the Fermi energy lies in the band. If the band is completely occupied or empty, no energy can be gained by band broadening.

Let us now consider the stability of the disordered local moment (DLM) (or spin-glass) state as compared to the ferromagnetic one. In the CPA-description of the DLM state, for a given Mn atom 50 % of the neighboring Mn atoms have a moment being parallel aligned to the central moment, and 50 % are antiferromagnetically aligned. The parallel aligned pairs lead, as in the ferromagnetic case, to a broadened impurity band, but with a reduced band width scaling as $\sqrt{c/2}$, since only 50 % of the pairs are parallel aligned. Therefore in total the double exchange due to band broadening always favors the ferromagnetic configuration.

The 50 % antiferromagnetically aligned pairs gain energy by super-exchange. The density of states in the gap of two Mn impurities with antiparallel aligned moments is schematically shown in Fig. 6. Note that the minority and majority peaks are exchanged for the two atoms. Since the wave functions with the same spin directions hybridise with each other, covalent bonding and antibonding hybrides are formed. From the energetic point of view it is important, that the lower bonding states are shifted to lower energies, while the higher antibonding states are shifted to higher energies. Thus energy is gained by super-exchange, if the Fermi energy is located between the two peaks or in the peaks, however not, if E_{F} is below or above both peaks. As can be shown, the energy gain is given by $c\frac{t^2}{IM}$, where t is the effective hopping matrix element and IM is the exchange splitting, given by the exchange integral I times the local moment M. It is linear in c, since the effects of several antiparallel aligned neighbours on the central atom superimpose on each other.

Thus in the case of impurity bands in the gap, double exchange favors the ferromagnetic config-

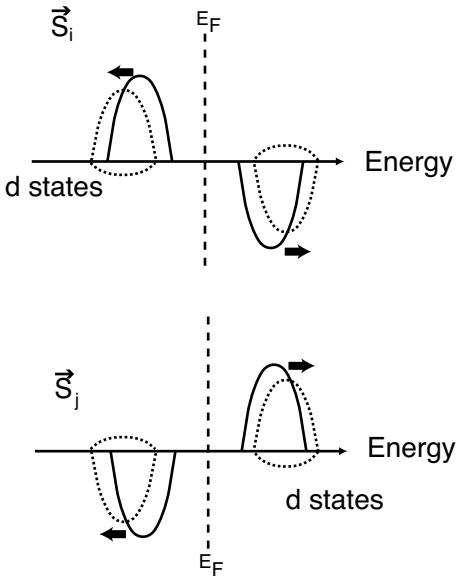

Figure 6: Super exchange: Shown are the local densities of states for two impurities with moments $\vec{S}_i$ = 'up' and $\vec{S}_j$ = 'down'. Due to hybridisation of the majority and the minority d-wavefunctions the lower energy levels are shifted to lower and the higher levels to higher energies as indicated by the dashed lines. Due to hybridisation also small peaks occur locally for the 'wrong' spin direction. The downward shift stabilises the antiferromagnetic alignment of the two local moments, provided the Fermi level falls between the two peaks, but not below or above.

uration and always wins, if the Fermi energy lies (well) in the band. Then the energy gain due to double exchange, scaling as $\sqrt{c}|t|$, is always larger than the energy gain due to super exchange, scaling like $c|t|^2/IM$. However if the Fermi energy lies between the two bands or lies close to the band edges, super exchange wins stabilising the disordered local moment state. Thus the system (Ga, Mn)N is expected to be a ferromagnet, while (Ga, Fe)N should be a disordered system, since the t-band is completely filled. For the same reason, in the II-VI compounds Cr impurities should favour the ferromagnetic state, but Mn impurities the DLM state.

However these considerations are only valid for impurity band systems. If the majority d-level lies below the valence p-states, as it is the case for (Ga, Mn)Sb in Fig. 1, then we have a different situation which is schematically sketched in Fig. 7. In the majority band the low lying d-states of Mn hybridise with the valence band p-states of Sb, and effectively push the majority valence band to higher energy. The opposite is true for the minority valence states being pushed by the empty minority d-states to lower energies. Thus the valence band becomes spin polarised, with a moment of $-1\mu_B$ per Mn atom, i.e., antiparallel to the Mn moment. The other Mn atoms gain energy by also aligning antiparallel to this host polarisation, thus leading to an indirect ferromagnetic coupling of the Mn-atoms. Due to the strong localisation of Mn d wavefunctions the direct d-d interaction is very small.

This kind of exchange interaction is called Zener's kinetic or p-d exchange and favours ferromagnetism. No energy gain is obtained in the DLM state, since the host polarisations induced by non-aligned Mn moments cancel each other.

All ab-initio calculations presented in the previous section are based on the local density ap-

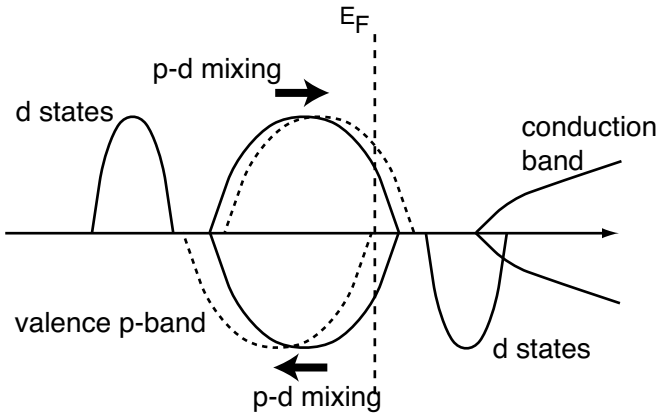

Figure 7: Kinetic p-d exchange: The low-lying 'localised' majority d-states hybridise with the majority valence p-band, pushing it up to higher energies as indicated by the dashed line. Analogously the empty minority d-level pushes the minority valence p-states to lower energies. Since due to charge neutrality the valence band must have one hole per Mn atom, this hole is confined to the majority band, leading to an Sb moment of $-1\mu_{\mathrm{B}}$ per Mn being antiferromagnetically aligned to the Mn-moments.

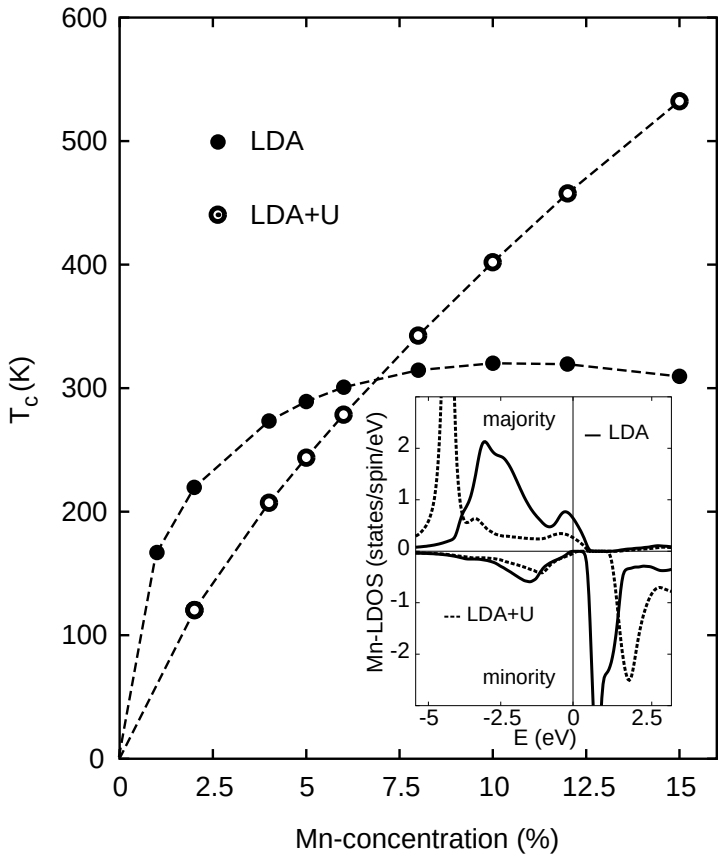

Figure 8: Meanfield Curie temperature of (Ga, Mn)As evaluated in the LDA and in the LDA+U approximation (with $U = 4$ eV). The inset shows the local density of states of the Mn atoms. Due to the Hubbard U of 4 eV, the Mn majority d-states are shifted to lower energies, while the resonance at the Fermi level is diminished. This increases the importance of p-d kinetic exchange and reduces the double exchange, so that T_{C} varies linear with concentration.

proximation (LDA). This approximation works in most cases very well, but has its limit for correlated systems. One typical error is, that the spin splitting is usually too small. The error can be partially removed by the LDA+U method, where U stands for the Hubbard U parameter of the Hubbard model. Fig. 8 shows the results of an LDA and LDA+U calculations for (Ga, Mn)As system with 5 % Mn. The inset shows the local Mn DOS in LDA and LDA+U, using a U parameter of $U = 4$ eV. As one sees, the U parameter of 4 eV shifts the majority peak by about 1.3 eV to lower energies, such that it is in good agreement with photoemission measurements [15, 16]. Since the d-states are now located in the lower region of the valence band, one expects that the p-d exchange becomes more dominant. The calculated Curie temperatures $T_{\mathrm{C}}^{\mathrm{MFA}}$ indeed show this effect. The LDA results show a $\sqrt{c}$-behavior resulting from double exchange, while the LDA+U results are more or less linear in c, indicating that in (Ga, Mn)As the kinetic p-d exchange is most important [13]. This exchange mechanism underlies all model calculations based on the Kondo Hamiltonian, which describe the physics of (Ga, Mn)As rather well. However the physics of the impurity band systems is very different and cannot be described by such a Hamiltonian (although this is very often done).

5 Exchange Coupling Constants and Curie Temperatures

The exchange coupling constants J_{ij} give according to eq. (7) the information about the orientational coupling between the local moments M_i and M_j. For the DMS-systems they have been calculated by embedding the two magnetic impurities i and j in the CPA medium of the ferromagnetic state, in this way including the substitutional disorder of all other impurities in an average way. As a result, the coupling constants are strongly concentration dependent due to the magnetic screening of the other impurities.

The calculated J_{ij} constants for (Ga, Mn)N, (Ga, Mn)P, (Ga, Mn)As and (Ga, Mn)Sb are shown in Fig. 9 for three different concentrations, i.e., 1 %, 5 % and 15 % of Mn impurities. The results show a qualitatively very different behaviour, in particular for the two extreme cases of (Ga, Mn)N and (Ga, Mn)Sb. In (Ga, Mn)N the interaction is very strong for the nearest neighbors, but the coupling of the further away atoms is very small. This is typical for the double exchange mechanism mediated by the impurity band. The coupling arises from the overlap of the impurity states on neighboring sites. Since these states are relatively well localised, the coupling is strong, but short ranged. (Ga, Mn)Sb represents the other extreme, the coupling of which is dominated by p-d exchange. Here the coupling is weak, but very long ranged. This arises from the large spatial extent of the Sb-p states near the valence band maximum, since the interaction is basically transferred by the spin polarised hole states at the Γ point.

The estimation of the Curie temperature T_{C} by the mean field expression $\frac{1}{3}c\sum_{i\neq 0} J_{0i}$ is very problematic for dilute systems with low concentrations, since it does not require any information on the interaction range. This simplification leads to significant errors in the calculations of T_{C} for low concentrations [17, 18]. It can be easily understood and is known as the percolation problem [19]. Let us consider a Heisenberg model with a ferromagnetic exchange interaction only between nearest neighbors (nearest neighbor Heisenberg model), and see what happens when the system is diluted with non-magnetic sites as schematically shown in Fig. 10-(a).

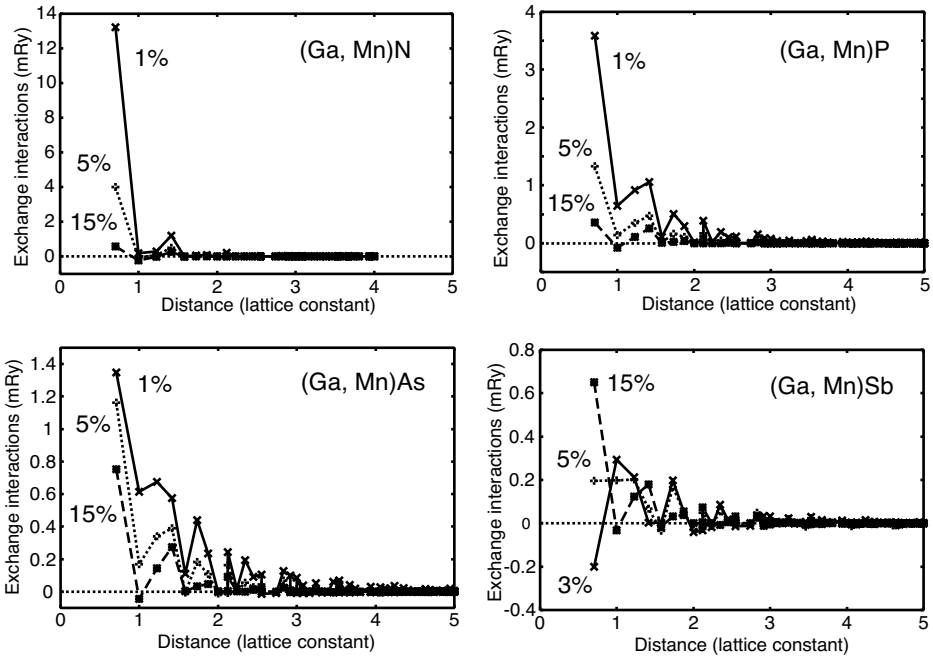

Figure 9: Exchange coupling constants J_{ij} between two Mn atoms as a function of the distance for three different concentrations. The concentration dependence arises from the screening effects of the other impurities, being described by the embedding of the two impurities in the CPA medium.

When the concentration of magnetic sites is 100 % , we have a perfect ferromagnetic network. Due to the dilution, the network is weakened, and for a concentration below a percolation threshold the ferromagnetism cannot spread all over the system leading to paramagnetic state since due to missing longer ranged interactions the moments can no longer align. Obviously this effect is not counted in the mean field equation for T_{C}, because the dilution effect is included only as a concentration factor c in the equation. In case of the nearest neighbor Heisenberg model, the percolation threshold c_p for the fcc structure is 20 % (note that the impurities sit on the fcc Ga sublattice of the zinc blende structure). In real systems such as (Ga, Mn)N the interaction reaches beyond the nearest neighbors and the real percolation threshold should be lower. However, below 20 % the strong nn coupling is not so important anymore, since only the much weaker longer ranged interaction induces the ferromagnetism, so that the Curie temperature is expected to drop considerably and to be much smaller than the mean field value, being determined to a large extent by the strong nn coupling J_{01}.

In order to take the percolation effect into account, we perform Monte Carlo simulation (MCS) for the classical Heisenberg model. The thermal average of magnetization M and its powers are calculated by means of the Metropolis algorithm [20]. Due to the finite size of super cells used in the simulation, it is difficult to determine T_{C} from the temperature dependence of $\langle M(T)\rangle$. In particular, when considering dilute systems, finite size effects and appropriate finite size scaling are of particular importance for a correct and efficient evaluation of T_{C} by Monte Carlo simulations. To avoid this difficulty, we use the cumulant crossing method proposed by Binder [20]. This method uses the finite size scaling in the forth order cumulant U_4 which is defined as $U_4 = 1 - \langle M^4\rangle/(\langle M^2\rangle)^2$. U_4 is calculated for various cell sizes and plotted as a function of

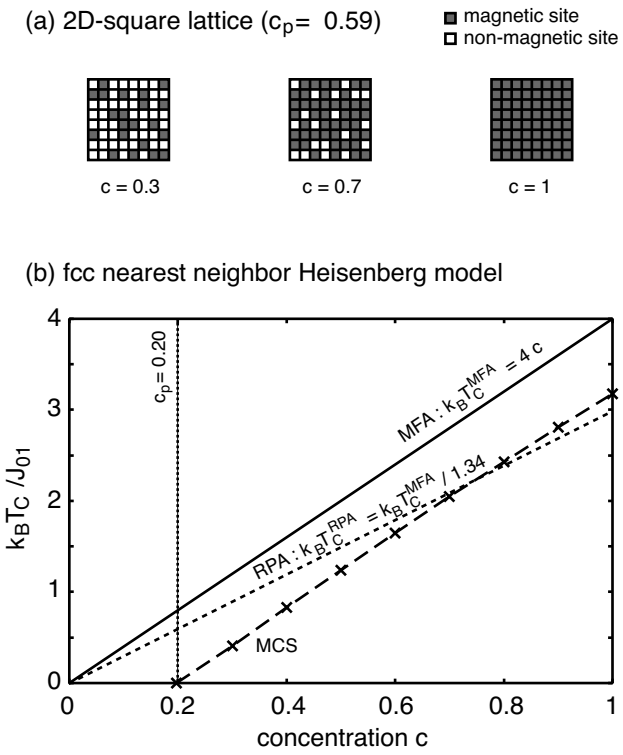

Figure 10: (a) Schematic picture of dilute 2-dimensional nearest neighgor Ising model in square lattice. The percolation thereshold is 0.59 in this case. (b) Curie temperatures of the classical nearest neighbour Heisenberg model for the fcc lattice as a function of the concentration. The full line gives the mean field results, being linear in c. The crosses connected by the dashed line give the exact values as obtained by Monte Carlo simulations (MCS), which vanish below the percolation threshold of $c_p = 20$ %. The nn coupling constant J_{01} has been fixed at a constant value.

temperature. If the cell size is larger than the correlation length, it can be shown that the $U_4(T)$ curves for different sizes cross each other at three characteristic temperatures. Two of them are $T = 0$ and $T = \infty$, and the other is $T = T_{\rm C}$. We use 3 cell sizes ($6 \times 6 \times 6, 10 \times 10 \times 10$ and $14 \times 14 \times 14$ conventional fcc cells) to carry out the cumulant crossing method for $T_{\rm C}$ calculations.

First, as a pedagogical example we show the calculated $T_{\rm C}$ for the dilute fcc nearest neighbour Heisenberg model as calculated by MFA and MCS in Fig. 10-(b). For MCSs for dilute systems, we take 30 different random configurations of magnetic sites for the ensemble average. As shown in Fig. 10-(b), it is found that the MFA gives a reasonable, but too high estimation of $T_{\rm C}$ for $c = 1$. However, with decreasing c both curves decline with nearly the same slope and below the percolation threshold, $c_p = 0.20$, the Curie temperature vanishes. Thus in the dilute concentration range below 20 %, which is most relevant for DMS systems, the failure of the MFA is evident [17, 18].

Next, we show the calculated $T_{\rm C}$ values of (Ga, Mn)N (Fig. 11-(a)) and (Ga, Mn)As (Fig. 11-(b)) as obtained by the MCS from the J_{ij} values in Fig. 9. Thirty configurations of Mn atoms are considered for averaging and J_{ij} interactions up to 15 shells are included. As shown in Fig. 11-(a), very small $T_{\rm C}$ values are predicted for low concentrations in (Ga, Mn)N. The MFA values are almost 2 orders of magnitude too large. Thus we find that the magnetism is

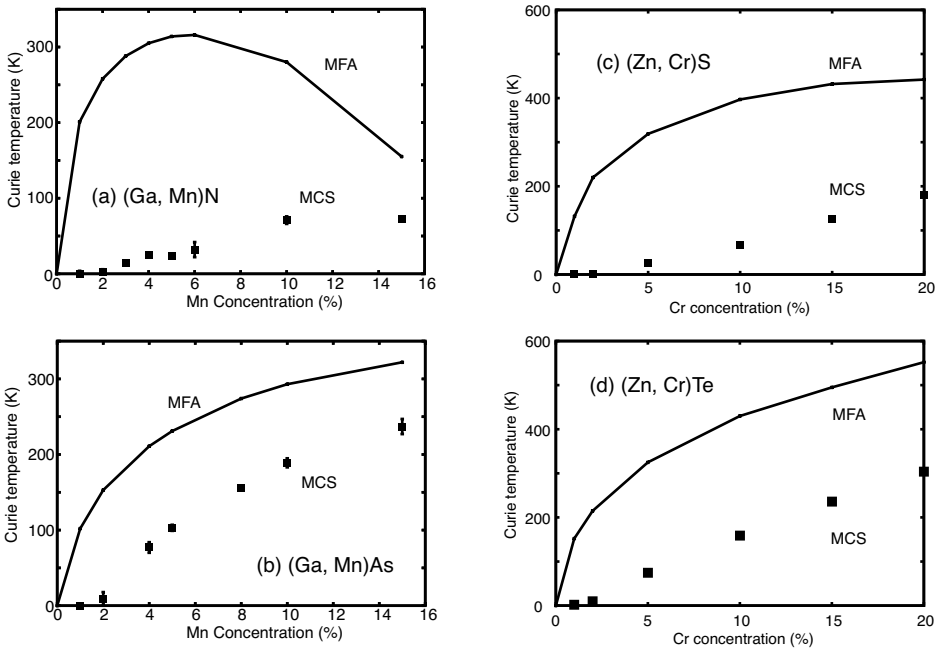

Figure 11: Curie temperatures of (a) (Ga, Mn)N, (b) (Ga, Mn)As, (c) (Zn, Cr)S and (d) (Zn, Cr)Te as evaluated in the mean field approximation (MFA) and by Monte Carlo simulations (MCS) from the J_{ij} values obtained in the LDA (see Fig. 9). Due to the percolation problem the Curie temperature of (Ga, Mn)N is strongly reduced for small concentrations. This effect can also be seen in (Zn, Cr)S and (Zn, Cr)Te. Due to the longer interaction range the reduction of Curie temperatures effect is more moderate in (Ga, Mn)As.

strongly suppressed due to the missing percolation of the strong nearest neighbour interactions. Only the weak, longer ranged interactions satisfy the percolation requirement, leading to small but finite Curie temperatures for 5, 10 and 15 % of Mn. As shown in Fig. 11-(b), due to the longer ranged interaction in (Ga, Mn)As, the reductions from the MFA are not very large, but still significant. Naturally these changes are larger for smaller concentrations. The T_{C} values of 103 K obtained for 5 % Mn is in good agreement with the experimental values of 118 K reported by Edmonds et al. [21]. This values refers to measurements in thin films which are free of Mn-interstitials representing double donors. Including interactions beyond 15th shell, MCS could give slightly higher T_{C} values for low concentrations. At very high concentrations we expect our results to increase towards the MFA values.

The experimental situation for T_{C} in (Ga, Mn)N is very controversial. There are many reports, where very high Curie temperatures, well above room temperature, have been observed, but also many observations of no ferromagnetism or only very low Curie temperatures. The above calculations suggest, that a homogeneously ferromagnetic phase with a Curie temperature around or above room temperature can be excluded. Therefore the experimentally observed very high T_{C} values have to be attributed to small ferromagnetic MnN clusters and segregated MnN phases, where the strong ferromagnetic nn interaction becomes fully effective.

The same method for calculating T_{C} is applied to (Zn, Cr)S and (Zn, Cr)Te as typical examples of II-VI DMS systems [22]. Results are shown in Fig. 11-(c) and -(d). In these compounds, impurity t-bands appear in the gap and 2/3 of the impurity bands are occupied (namely, they

are equivalent to Mn-doped III-V DMS such as (Ga, Mn)N from electron occupation point of view), therefore the double exchange is dominant mechanism. As a result, MFA values of T_C show $\sqrt{c}$ dependence. For both cases, MCS values of T_C deviate very much from MFA values due to the same reason in the case of (Ga, Mn)N. The suppression of the ferromagnetism in (Zn, Cr)S at small concentrations is as significant as in (Ga, Mn)N. The effect is slightly moderate in (Zn, Cr)Te than in (Zn, Cr)S, because ZnTe has smaller band gap than ZnS and the Cr t-band is very near to the host valence band in (Zn, Cr)Te [22]. Calculated exchange interactions of (Zn, Cr)Te are short ranged but not as short as in (Ga, Mn)N. The observation of a T_C value of 300 K for (Zn, Cr)Te with 20 % Cr is in good agreement with MCS results. The linear scaling in MCS values of T_C in Fig. 11-(d) has been observed in recent experiments [23, 24]

6 Summary

Due to their half-metallicity and structural similarity to semiconductors dilute magnetic semiconductors are hopeful materials for a future spintronics. However the Curie temperatures are in general very low. In this review we have discussed the origin of ferromagnetism in these materials and presented ab-initio calculations for the electronic and magnetic properties of (Ga, Mn)N, (Ga, Mn)P, (Ga, Mn)As and (Ga, Mn)Sb. The results point of the existence of two classes of DMS with very different properties:

(i) In systems with localised majority d-states deep in the valence band such as (Ga, Mn)As and (Ga, Mn)Sb, the ferromagnetism is induced by Zener's p-d exchange, leading to holes in the majority p-valence band. This interaction is relatively weak, but long ranged. At small concentrations the Curie temperature is only moderately reduced by the percolation effect.

(ii) In systems with impurity-bands in the band gap such as (Ga, Mn)N and (Zn, Cr)Te, the ferromagnetism is driven by Zener's double exchange. Here the magnetic coupling is strong, but short ranged. Therefore, in the dilute limit the ferromagnetism is strongly suppressed, since percolation of the strong nearest neighbor interactions cannot be achieved.

A way to achieve higher Curie temperatures might be to try to increase the impurity concentration. For the p-d systems this should help, since the Curie temperature basically scales linearly with the concentration. For the impurity band systems the percolation effects become less important at higher concentrations, so also here higher concentrations would help. The observation of the T_C of 300 K for 20 % Cr doped ZnTe supports this argument [23, 24].

References

[1] F. Matsukura, H. Ohno and T. Dietl, *Hand book of Magnetic Materials*, **14** (Elsevier, Amsterdam, 2002).

[2] Special issue: *Semiconductor Spintronics* in J. Semicond. Sci. Technol, **17** 275-403 (2002).

[3] R. A. de Groot, F. M. Mueller, P. G. van Engen and K. H. J. Buschow, Phys. Rev. Lett. **50** 2024 (1983).

[4] R. J. Soulen Jr., J. M. Byers, M. S. Osofsky, B. Nadgorny, T. Ambrose, S. F. Cheng, P. R. Broussard, C. T. Tanaka, J. Nowak, J. S. Moodera, A. Barry and J. M. D. Coey, Science **282** 85 (1988).

[5] H. Kato, T. Okuda, Y. Okimoto, Y. Tomioka, K. Oikawa, T. Kamiyama and Y. Tokura, Phys. Rev. B **69** 184412 (2004).

[6] H. Ohno, H. Munekata, T. Penney, S. von Molnar, L. L. Chang, Phys. Rev. Lett. **68** 2664 (1992).

[7] H. Ohno, A. Shen, F. Matsukura, A. Oiwa, A. Endo, S. Katsumoto and Y. Iye, Appl. Phys. Lett. **69** 363 (1996).

[8] S. A. Wolf, D. D. Awschalom, R. A. Buhrman, J. M. Daughton, S. von Molnar, M. L. Roukes, A. Y. Chtchelkanova and D. M. Treger, Science **294** 1488 (2001).

[9] H. Akai and P. H. Dederichs, Phys. Rev. B **47** 8739 (1993).

[10] H. Akai, Department of Physics, Graduate School of Science, Osaka University, Machikaneyama 1-1, Toyonaka 560-0043, Japan, akai@phys.sci.osaka-u.ac.jp (2000)

[11] A. I. Liechtenstein et al., J. Magn. Magn. Matter **67** 65 (1987).

[12] K. Sato, P. H. Dederichs and H. Katayama-Yoshida, Europhys. Lett. **61** 403 (2003).

[13] K. Sato, P. H. Dederichs, H. Katayama-Yoshida and J. Kudrnovsky, J. Phys. Condens. Matt. **16** S5491 (2004).

[14] H. Akai, Phys. Rev. Lett. **81** 3002 (1998).

[15] J. Okabayashi et al., Phys. Rev. B **59** R2486 (1999).

[16] O. Rader et al., Phys. Rev. B **69** 075202 (2004).

[17] K. Sato, W. Schweika, P. H. Dederichs and H. Katayama-Yoshida, Phys. Rev. B **70** 201202 (2004).

[18] L. Bergqvist, O. Eriksson, J. Kudrnovsky, V. Drchal, P. Korzhavyi and I. Turek, Phys. Rev. Lett. **93** 137202 (2004).

[19] D. Stauffer and . Aharony, *Introduction to Percolation Theory* (Taylor and Francis, Philadelphia, 1994).

[20] K. Binder and D. W. Heerman, *Monte Carlo Simulations in Statistical Physics* (Springer, Berlin, 2002).

[21] K. W. Edmonds et al., Appl. Phys. Lett. **81** 4991 (2002).

[22] T. Fukushima, K. Sato, H. Katayama-Yoshida and P. H. Dederichs, Jpn. J. Appl. Phys. **43** L1416 (2004).

[23] H. Saito, V. Zayets, S. Yamagata and K. Ando, J. Appl. Phys. **95** 7175 (2004).

[24] N. Ozaki, N. Nishizawa, K.-T. Nam, S. Kuroda and K. Takita, Phys. Status Solidi C **1** 957 (2004).